Filling the gaps

Alex Lipton and Artur Sepp
Bank of America Merrill Lynch
alex.lipton@baml.com
artur.sepp@baml.com

Current version 10/06/2011

Abstract

The calibration of local volatility models to market data is one of the most fundamental problems of financial engineering. Under the restrictive assumption that the *entire* implied volatility surface is known, this problem can be solved by virtue of the so-called Dupire equation. In reality, however, the number of available data points is very limited and construction of a non-arbitrageable implied volatility surface is difficult, if not impossible, since it requires both *interpolation* and *extrapolation* of the market data. Thus, it is more natural to build the local volatility surface directly. In this article we present a generic semi-analytical approach to calibrating a parametric local volatility surface to the market data in the realistic case when this data is sparse. This approach also allows one to build a non-arbitrageable implied volatility surface. The power of the method is illustrated by considering layered local volatility and generating local and implied volatility surfaces for options on SX5E.

1 Introduction

Some of the most fundamental and long considered solved problems of financial engineering, such as construction of yield curves, calibration of implied volatility surfaces, etc., have recently turned out to be more complex than previously thought. In particular, it has become apparent that one of the principal challenges of options pricing and risk-management is the sparseness of market data for model calibration and, in the case of severe market dislocations, its extreme behavior. The fact that options markets are not nearly as liquid as is conventionally thought was especially clear during the most recent financial upheaval. A case in point is Table 1, which shows actual market quotes for options on SX5E, often thought of as very liquid. It is obvious that market quotes are very sparse in both strike and maturity directions. As the spot price moves, options which were close to at-the-money at inception become illiquid, so that one has to find ways to interpolate and extrapolate the implied volatilities of liquid options to mark them to market. Moreover, for certain asset classes the

concept of implied volatility surface is ill-defined. For instance, for commodities it is not uncommon to have market prices of options for a single maturity, while for forex it is customary to quote option prices with no more than five values of delta and very few maturities.

The calibration of a model to sparse market data is needed not only for the consistent pricing of illiquid vanilla options, but also for the valuation of exotic options. The latter is particularly demanding since it requires the construction of the implied and local volatility surfaces across a wide range of option strikes and maturities.

The calibration problem has attracted much attention over the years, see, e.g., Ayache *et al.* (2004). The conventional approach to the calibration problem is to choose a functional form for the implied volatility across strikes and then to calibrate the parameters of the function to liquid option prices at available maturities, assuming that these parameters are piece-wise constant or piece-wise linear in maturity. While this elementary approach is quite easy to implement, it has severe drawbacks, which are particularly apparent when market quotes are sparse. By its very nature, it requires both interpolation and extrapolation, so that ensuring that vanilla option prices are non-arbitrageable across strikes and maturities, the implied volatility in the wings is well-defined, etc., is often impossible. A case in point is the well-known SABR model (Hagan *et al.*, 2002) which under current market conditions routinely produces arbitrageable implied volatility surfaces. Nevertheless, assuming that the above mentioned difficulties are somehow overcome, and a "high quality" implied volatility surface is properly constructed, the local volatility surface can be built using the Dupire formula (Dupire, 1994). Additional insights can be found in Derman & Kani (1994), Rubinstein (1994), and Andersen & Brotherton-Ratcliffe (1998), among others.

An alternative approach is to choose a functional form for the local volatility, calculate the corresponding option prices for a set of strikes and maturities, and select parameters to fit the market quotes. Parametric models of this type include the CEV model (Cox, 1975), displaced diffusion model (Rubinstein, 1983), hyperbolic tangent model (Brown & Randall, 1999), hyperbolic model (Lipton, 2002), and stochastic local volatility models (Blacher, 2001, Hagan *et al.*, 2002, and Lipton, 2002). In general, these models lack the flexibility to fit the entire volatility surface exactly because they use a limited number of parameters. Thus, such models require least-squares error minimization to achieve reasonable calibration. Calibration using a flexible parametric form for the local volatility with sufficient number of time-dependent parameters is considered by Coleman *et al.* (1999), and Andreasen & Huge (2010) (thereafter AH for brevity) among others.

This investigation is inspired in part by the work of AH, who choose a tiled local volatility function. They use a fully implicit finite-difference scheme to compute the probability density of the underlying, stepping forward in time and calibrating model parameters by a least-squares algorithm. Since the size of time step is determined by market quotes, it cannot be reduced arbitrarily, so that, while very instructive, the AH method clearly has limited accuracy. More-

over, its accuracy cannot be easily improved because the chosen discretization technique is an integral part of the algorithm itself.

This article proposes a new semi-analytic method allowing one to calibrate a model with tiled local volatility to sparse market data by using the direct and inverse Laplace transforms. Mathematically speaking, this method reduces the solution of partial differential equations (PDEs) to the solution of several ordinary differential equations (ODEs). By its very nature this method is very accurate and does not suffer from any of the drawbacks of the original AH technique, while retaining all of its advantages. Moreover, it can be applied in a much more general setting provided that solutions of the corresponding ODEs can be found analytically, as in e.g. piecewise CEV, displaced-diffusion, and hyperbolic volatility models. The main idea is to have a parametric form for the local volatility with as many parameters as there are market quotes. This allows one to find an exact solution to the calibration problem at each forward time step, rather than to solve it in the least-squares sense.

For illustration purposes, the method is applied in the case of tiled local volatility, and local and implied volatility surfaces for options on SX5E are generated. To facilitate comparisons with the AH technique, the same set of data is used. By construction, the corresponding implied volatility surface is non-arbitrageable and has regular behavior in the wings.

The method described in this paper is based on an idea originally presented by one of the authors at the Global Derivatives Conference in Paris (Lipton, 2011). The technique of the inverse and direct Laplace transform, which is central to the method, is classical in nature. Some of the current results can be traced back to the work on the propagation of heat in tiled media (see, e.g., Leij & van Genuchten, 1995, among many others). It is worth mentioning that in the latter work time-dependent parameters are not considered.

2 Generic calibration problem

For regular diffusion processes, the generic calibration problem reduces to defining the local volatility in such a way that market quotes for the corresponding option prices coincide with model prices. In this paper it is assumed that interest rates are deterministic; for brevity they are set to zero. The calibration problem for local volatility of the one-dimensional diffusion is represented by the Dupire equation (Dupire, 1994) for call prices $C(T,K)$ as functions of maturity time T and strike K:

$$\begin{array}{c} C_T - \frac{1}{2}\sigma_{loc}^2(T,K)\,K^2 C_{KK} = 0, \\ C(0,K) = (S-K)_+ \end{array} \tag{1}$$

If market call prices $C(T,K)$ are known *for all* T,K, then $\sigma_{loc}^2(T,K)$ can found by inverting equation (1):

$$\sigma_{loc}^2(T,K) = \frac{2C_T(T,K)}{K^2 C_{KK}(T,K)}. \tag{2}$$

If instead $\sigma_{loc}^2(T,K)$ is given by a particular functional form, prices of call options have to be obtained by solving equation (1). The resulting calibration problem is solved in the least-squares sense. While the Dupire equation (1) is one of the most ruthlessly efficient equations in the entire financial engineering field, most of the time the highly stylized equation (2) is used instead. In view of the fact that under normal conditions $C(T,K)$ are known *only for a few* T_i, K_j, this usage is hard to justify.

For computational purposes, it is more convenient to deal with covered calls $\bar{C}(T,K) = S - C(T,K)$, which solve the following problem

$$\begin{array}{c} \bar{C}_T - \frac{1}{2}\sigma_{loc}^2(T,K)\,K^2\bar{C}_{KK} = 0, \\ \bar{C}(0,K) = S - (S-K)_+ . \end{array} \tag{3}$$

Equation (3) is simplified by introducing a new independent variable X, $X = \ln(K/S)$, and a new dependent variable $B(T,X)$, $\bar{C}(T,X) = Se^{X/2}B(T,X)$. The transformed pricing problem is written as follows

$$\begin{array}{c} B_T(T,X) - \frac{1}{2}v(T,X)\left(B_{XX}(T,X) - \frac{1}{4}B(T,X)\right) = 0, \\ B(0,X) = e^{X/2}\mathbf{1}_{\{X\le 0\}} + e^{-X/2}\mathbf{1}_{\{X>0\}}, \end{array} \tag{4}$$

where $v(T,X) = \sigma_{loc}^2\left(T, Se^X\right)$. Its solution can be represented as follows:

$$B(T,X) = \int_{-\infty}^{\infty} G(T,X,X')B(0,X')dX',$$

where $G(T,X,X')$ is the Green's function that solves equation (4) with initial condition given by delta function: $\delta(X-X')$. Here X is a forward variable and X' is a backward variable.

From now on, it is assumed that v is a piece-wise constant function of time,

$$v(T,X) = v_i(X), \qquad T_{i-1} < T \le T_i, \qquad 1 \le i \le I,$$

so that equation (4) can be solved by induction. On each time interval $T_{i-1} < T \le T_i$, $1 \le i \le I$, the corresponding problem is represented in the form

$$\begin{array}{c} B_{i,\tau}(\tau,X) - \frac{1}{2}v_i(X)\left(B_{i,XX}(\tau,X) - \frac{1}{4}B_i(\tau,X)\right) = 0, \\ B_i(0,X) = B_{i-1}(X), \end{array} \tag{5}$$

where

$$B_i(\tau,X) = B(T,X), \qquad \tau = T - T_{i-1}, \qquad B_{i-1}(X) = B(T_{i-1},X).$$

Induction starts with

$$B_0(X) = e^{X/2}\mathbf{1}_{\{X\le 0\}} + e^{-X/2}\mathbf{1}_{\{X>0\}}.$$

The solution of problem (5) can be written as

$$B_i(\tau,X) = \int_{-\infty}^{\infty} G_i(\tau,X,X')B_{i-1}(X')\,dX', \tag{6}$$

where G_i is the corresponding Green's function for the corresponding time interval.

As a crude approximation, the time-derivative $\partial/\partial\tau$ can be implicitly discretized and forward problem (5) can be cast in the form

$$B_i^{AH}(X) - \frac{1}{2}(T_i - T_{i-1})\, v_i(X)\left(B_{i,XX}^{AH}(X) - \frac{1}{4}B_i^{AH}(X)\right) = B_{i-1}^{AH}(X),$$

where $B_i^{AH}(X) \approx B(T_i, X)$. This is the approach chosen by AH in the specific case of piecewise constant $v_i(X)$. While intuitive and relatively simple to implement, this approach is not accurate, by its very nature, and its accuracy cannot be improved. Moreover, for every τ, $0 < \tau \leq T_i - T_{i-1}$, a separate equation single step equation from time T_{i-1} to $T_{i-1} + \tau$ has to be solved. These equations are solved in isolation and are not internally consistent. Below an alternative approach is proposed. This approach is based on representation (6); by construction it is exact in nature.

3 Solution of the calibration problem via the Laplace transform

In this section a classical and powerful integral transform technique is used for solving problem (5). It turns out that it can be solved exactly, rather than approximately, via the direct and inverse Laplace transform (for applications of the Laplace transform in derivatives pricing see Lipton, 2001). After performing the direct Carson-Laplace transform

$$\hat{B}_i(\lambda, X) = \lambda \mathfrak{L}\{B_i(\tau, X)\},$$

the following Sturm-Liouville problem is obtained:

$$\begin{gathered}\hat{B}_i(\lambda, X) - \tfrac{1}{2}\tfrac{1}{\lambda} v_i(X)\left(\hat{B}_{i,XX}(\lambda, X) - \tfrac{1}{4}\hat{B}_i(\lambda, X)\right) = B(T_{i-1}, X), \\ \hat{B}_i(\lambda, X) \underset{X\to\pm\infty}{\to} 0.\end{gathered} \tag{7}$$

It is clear that

$$B_i^{AH}(X) = \hat{B}_i\left(\frac{1}{T_i - T_{i-1}}, X\right). \tag{8}$$

It is convenient to represent equation (7) in the standard Sturm-Liouville form

$$\begin{gathered}-\hat{B}_{i,XX}(\lambda, X) + q_i^2(\lambda, X)\,\hat{B}_i(\lambda, X) = \left(q_i^2(\lambda, X) - \tfrac{1}{4}\right) B(T_{i-1}, X), \\ \hat{B}_i(\lambda, X) \underset{X\to\pm\infty}{\to} 0,\end{gathered}$$

where

$$q_i^2(\lambda, X) = \frac{2\lambda}{v_i(X)} + \frac{1}{4}.$$

The corresponding Green's function $\hat{G}_i(\lambda, X, X')$ solves the following adjoint Sturm-Liouville problems

$$\begin{gathered}-\hat{G}_{i,XX}(\lambda, X, X') + q_i^2(\lambda, X)\hat{G}_i(\lambda, X, X') = \delta(X - X'), \\ \hat{G}_i(\lambda, X, X') \underset{X\to\pm\infty}{\to} 0, \\ -\hat{G}_{i,X'X'}(\lambda, X, X') + q_i^2(\lambda, X')\hat{G}_i(\lambda, X, X') = \delta(X - X'), \\ \hat{G}_i(\lambda, X, X') \underset{X'\to\pm\infty}{\to} 0.\end{gathered} \tag{9}$$

To be concrete, backward problem (9) is considered and its fundamental solutions are denoted by $\hat{g}_i^{\pm}(\lambda, X')$:

$$-\hat{g}_{i,X'X'}^{\pm}(\lambda, X') + q_i^2(\lambda, X')\hat{g}_i^{\pm}(\lambda, X') = 0, \qquad \hat{g}_i^{\pm}(\lambda, X') \underset{X'\to\pm\infty}{\to} 0.$$

These solutions are unique (up to a constant). It is well-known (see, e.g., Lipton (2001)) that

$$\hat{G}_i(\lambda, X, X') = \frac{1}{W(\lambda)} \begin{cases} \hat{g}_i^{+}(\lambda, X)\hat{g}_i^{-}(\lambda, X'), & X' \le X, \\ \hat{g}_i^{-}(\lambda, X)\hat{g}_i^{+}(\lambda, X'), & X' > X, \end{cases}$$

where $W(\lambda)$ is the so-called Wronskian:

$$W(\lambda) = \hat{g}_i^{-}(\lambda, X)\hat{g}_{i,X'}^{+}(\lambda, X') - \hat{g}_i^{+}(\lambda, X)\hat{g}_{i,X'}^{-}(\lambda, X').$$

Once the Green's function is found, the solution of equation (7) can be represented in the form

$$\hat{B}_i(\lambda, X) = \int_{-\infty}^{\infty} \hat{G}_i(\lambda, X, X')\left(q_i^2(\lambda, X') - \frac{1}{4}\right) B_{i-1}(X')\, dX'. \tag{10}$$

This is a generic formula for the computation of one-step option prices in models where the Green's function $\hat{G}(\lambda, X, X')$ is known in the closed form. In applications, the Laplace transform $\hat{G}(\lambda, X, X')$ and the corresponding integral will be calculated explicitly. The inverse Carson-Laplace transform yields $B(T_{i-1} + \tau, X)$ for $0 < \tau \le T_i - T_{i-1}$, including $B_i(X)$. In order to compute the integral in equation (10) it is assumed that X and X' are defined on the same grid $X_{\min} < X < X_{\max}$ and the trapezoidal rule is applied.

Once $B_i(X)$ is computed for a given $v_i(X)$, the latter function is changed until market prices are reproduced. The latter operation is non-linear in nature and might or might not be feasible. This depends predominantly on whether or not market prices are internally consistent.

To summarize, in this section an abstract exact solution to the generic calibration problem has been developed. By construction, the corresponding volatility surface is smooth and non-arbitrageable.

4 Calibration problem for a tiled local volatility case

In this section, the generic calibration method developed in the previous section is applied to the case of tiled local volatility considered by AH. Assuming that a *discrete* set of market call prices $C_{mrkt}(T_i, K_j)$, $0 \le i \le I$, $0 \le j \le J_i$, is known, a tiled local volatility $\sigma_{loc}(T, K)$ of the form

$$\sigma_{loc}(T,K) = \sigma_{ij}, \quad T_{i-1} < T \le T_i, \quad \bar{K}_{j-1} < K \le \bar{K}_j, \quad 1 \le i \le I, \quad 0 \le j \le J_i,$$
$$\bar{K}_{-1} = 0, \quad \bar{K}_j = \tfrac{1}{2}(K_j + K_{j+1}), \quad 0 \le j \le J_i - 1, \quad \bar{K}_{J_i} = \infty,$$

is considered. Clearly, non-median break points can be chosen if needed. Equivalently, $\sigma_{loc}(T, X)$ has the form

$$\sigma_{loc}(T,X) = v_{ij}, \quad T_{i-1} < T \le T_i, \quad \bar{X}_{j-1} < X \le \bar{X}_j, \quad \bar{X}_j = \ln\left(\bar{K}_j/S\right).$$

By construction, for every T_i, $\sigma_{loc}(T_i, K)$ depends on as many parameters as there are market quotes. On every step of the calibration procedure these parameters are adjusted in such way that the corresponding model prices $C_{mdl}(T_i, K_j)$ and market prices $C_{mrkt}(T_i, K_j)$ coincide within prescribed accuracy.

Consider problem (9). For calibration it is sufficient to consider $X = X_j$, where $X_j = \ln(S_j/K)$; however, to propagate the solution forward from T_{i-1} to T_i, it is necessary to consider all X. A new set of ordered points is introduced

$$\{Y_k\} = \left\{\bar{X}_j\right\} \cup X, \quad -1 \le k \le J_1 + 1, \quad Y_{-1} = -\infty, \quad Y_{J_1+1} = \infty,$$

and it is assumed that $X = Y_{k^*}$. On each interval

$$\mathcal{J}_k = \{X' | \, Y_{k-1} \le X' \le Y_k\},$$

except for the first and the last one, the general solution of equation (9) has the form

$$g_k(X') = \alpha_{k,+} e^{q_k\left(X' - Y_{k^*}\right)} + \alpha_{k,-} e^{-q_k\left(X' - Y_{k^*}\right)},$$

while on the first and last intervals it has the form

$$g_0(X') = \alpha_{0,+} e^{q_0\left(X' - Y_{k^*}\right)}, \quad g_{J_1+1}(X') = \alpha_{J_1+1,-} e^{-q_{J_1+1}\left(X' - Y_{k^*}\right)},$$

so that the corresponding Green's function decays at infinity. Here q_k are constant values of the potential on the corresponding interval. For $k \ne k^*$ both $\hat{G}$ and $\hat{G}_X$ have to be continuous, while for $k = k^*$ only $\hat{G}$ is continuous, while $\hat{G}_X$ has a jump of size -1. Thus, the following system of $2(J_1 + 1)$ linear equations can be obtained:

$$\begin{pmatrix} -E^+_{kk} & -E^-_{kk} & E^+_{k+1k} & E^-_{k+1k} \\ -q_k E^+_{kk} & q_k E^-_{kk} & q_{k+1} E^+_{k+1k} & -q_{k+1} E^-_{k+1k} \end{pmatrix} \begin{pmatrix} \alpha_{k,+} \\ \alpha_{k,-} \\ \alpha_{k+1,+} \\ \alpha_{k+1,-} \end{pmatrix} = \begin{pmatrix} 0 \\ -\delta_{kk^*} \end{pmatrix}.$$

Here

$$E_{kl}^{\pm} = e^{\pm q_k (Y_l - Y_{k^*})},$$

and δ_{kk^*} is the Kronecker symbol. In matrix form these equations can be written as

$$\mathcal{R}\vec{A} = \vec{B}_{k^*}, \tag{11}$$

For instance, for $J = 3, k^* = 1$, we have

$$\mathcal{R} = \begin{pmatrix}
-E_{00}^{+} & E_{10}^{+} & E_{10}^{-} & & & & & & \\
-q_0 E_{00}^{+} & q_1 E_{10}^{+} & -q_1 E_{10}^{-} & & & & & & \\
 & -1 & -1 & 1 & 1 & & & & \\
 & -q_1 & q_1 & q_2 & -q_2 & & & & \\
 & & & -E_{22}^{+} & -E_{22}^{-} & E_{32}^{+} & E_{32}^{-} & & \\
 & & & -q_2 E_{22}^{+} & q_2 E_{22}^{-} & q_3 E_{32}^{+} & -q_3 E_{32}^{-} & & \\
 & & & & & -E_{33}^{+} & -E_{33}^{-} & E_{43}^{-} & \\
 & & & & & -q_3 E_{33}^{+} & q_3 E_{33}^{-} & -q_4 E_{43}^{-}
\end{pmatrix},$$

$$\vec{A} = \begin{pmatrix} \alpha_{0,+} & \alpha_{1,+} & \alpha_{1,-} & \alpha_{2,+} & \alpha_{2,-} & \alpha_{3,+} & \alpha_{3,-} & \alpha_{4,-} \end{pmatrix}^T,$$

$$\vec{B}_{k^*} = \begin{pmatrix} 0 & 0 & 0 & -1 & 0 & 0 & 0 & 0 \end{pmatrix}^T,$$

Although matrix equation (11) is five-diagonal (rather than tri-diagonal), it can still be solved very efficiently via forward elimination and backward substitution. First, $(\alpha_{1,+}, \alpha_{1,-})^T$ is eliminated in favor of $\alpha_{0,+}$ and $(\alpha_{J,+}, \alpha_{J,-})^T$ is eliminated in favor of $\alpha_{J+1,-}$:

$$\begin{pmatrix} \alpha_{1,+} \\ \alpha_{1,-} \end{pmatrix} = \frac{1}{2q_1} \begin{pmatrix} (q_1 + q_0) E_{10}^{-} E_{00}^{+} \\ (q_1 - q_0) E_{10}^{+} E_{00}^{+} \end{pmatrix} \alpha_{0,+} \equiv \vec{C}_1 \alpha_{0,+},$$

$$\begin{pmatrix} \alpha_{J,+} \\ \alpha_{J,-} \end{pmatrix} = \frac{1}{2q_J} \begin{pmatrix} (q_J - q_{J+1}) E_{JJ}^{-} E_{J+1J}^{-} \\ (q_J + q_{J+1}) E_{JJ}^{+} E_{J+1J}^{-} \end{pmatrix} \alpha_{J+1,-} \equiv \vec{D}_J \alpha_{J+1,-},$$

Next, $(\alpha_{k,+}, \alpha_{k,-})^T$ is eliminated in favor of $(\alpha_{k-1,+}, \alpha_{k-1,-})^T$, $2 \le k \le k^*$ and $(\alpha_{k,+}, \alpha_{k,-})^T$ is eliminated in favor of $(\alpha_{k+1,+}, \alpha_{k+1,-})^T$, $k^* + 1 \le k \le J - 1$:

$$\begin{pmatrix} \alpha_{k,+} \\ \alpha_{k,-} \end{pmatrix} = \frac{1}{2q_k} \begin{pmatrix} (q_k + q_{k-1}) E_{kk-1}^{-} E_{k-1k-1}^{+} & (q_k - q_{k-1}) E_{kk-1}^{-} E_{k-1k-1}^{-} \\ (q_k - q_{k-1}) E_{kk-1}^{+} E_{k-1k-1}^{+} & (q_k + q_{k-1}) E_{kk-1}^{+} E_{k-1k-1}^{-} \end{pmatrix} \begin{pmatrix} \alpha_{k-1,+} \\ \alpha_{k-1,-} \end{pmatrix} \equiv \mathcal{S}_k \begin{pmatrix} \alpha_{k-1,+} \\ \alpha_{k-1,-} \end{pmatrix}$$

$$\begin{pmatrix} \alpha_{k,+} \\ \alpha_{k,-} \end{pmatrix} = \frac{1}{2q_k} \begin{pmatrix} (q_k + q_{k+1}) E_{kk}^{-} E_{k+1k}^{+} & (q_k - q_{k+1}) E_{kk}^{-} E_{k+1k}^{-} \\ (q_k - q_{k+1}) E_{kk}^{+} E_{k+1k}^{+} & (q_k + q_{k+1}) E_{kk}^{+} E_{k+1k}^{-} \end{pmatrix} \begin{pmatrix} \alpha_{k+1,+} \\ \alpha_{k+1,-} \end{pmatrix} \equiv \mathcal{T}_k \begin{pmatrix} \alpha_{k+1,+} \\ \alpha_{k+1,-} \end{pmatrix},$$

and a recursive set of vectors is computed

$$\vec{C}_k = \mathcal{S}_k \vec{C}_{k-1}, \quad 2 \le k \le k^*, \qquad \vec{D}_k = \mathcal{T}_k \vec{D}_{k+1}, \quad k^* + 1 \le k \le J - 1.$$

Finally, a system of 2×2 equations for $\alpha_{0,+}, \alpha_{J+1,-}$ is obtained and solved

$$\begin{pmatrix} -1 & -1 \\ -q_{k^*} & q_{k^*} \end{pmatrix} \vec{C}_{k^*} \alpha_{0,+} + \begin{pmatrix} 1 & 1 \\ q_{k^*+1} & -q_{k^*+1} \end{pmatrix} \vec{D}_{k^*+1} \alpha_{J+1,-} = \begin{pmatrix} 0 \\ -1 \end{pmatrix}. \tag{12}$$

Once $\alpha_{0,+}, \alpha_{J+1,-}$ are determined, $(\alpha_{k,+}, \alpha_{k,-})^T$ are calculated by using vectors $\vec{C}_k$ or $\vec{D}_k$. This procedure is just icing on the cake since the size of the corresponding system (determined by the number of market quotes) is quite small, and is not directly related to the size of the interpolation grid.

Once the coefficient vector $\vec{A}$ is known, $\hat{B}_i(\lambda, X)$ can be computed semi-analytically via equation (10):

$$\begin{array}{c} \hat{B}_i(\lambda,X) = \left(q_0^2 - \frac{1}{4}\right)\alpha_{0,+} e^{-q_0 Y_{k^*}} \int_{-\infty}^{Y_0} e^{q_0 X'} B_{i-1}(X')\, dX' \\ + \sum_{k=1}^{J_i} \left(q_k^2 - \frac{1}{4}\right) \left(\alpha_{k,+} e^{-q_k Y_{k^*}} \int_{Y_{k-1}}^{Y_k} e^{q_k X'} B_{i-1}(X')\, dX' \right. \\ \left. + \alpha_{k,-} e^{q_k Y_{k^*}} \int_{Y_{k-1}}^{Y_k} e^{-q_k X'} B_{i-1}(X')\, dX' \right) \\ + \left(q_{J_i+1}^2 - \frac{1}{4}\right) \alpha_{J_i+1,-} e^{q_{J_{i+1}} Y_{k^*}} \int_{Y_{J_1}}^{\infty} e^{-q_{J_{i+1}} X'} B_{i-1}(X')\, dX'. \end{array} \tag{13}$$

The corresponding integrals are computed via the trapezoidal rule. Variables X and X' are defined on the same dense spatial grid $X_{\min} < X, X' < X_{\max}$; this grid is similar to the one used in a conventional finite-difference solver. For $X' > X_{\max}$ or $X' < X_{\min}$ it is assumed that $B_{i-1}(X') = e^{-|X|/2}$. Since these integrals are independent on Y_{k^*}, they can be pre-computed for all X; as a result, the corresponding calculation has complexity linear in J_i. It is worth noting that for $i = 1$, the corresponding integrals can be computed analytically.

The inverse Carson-Laplace transform generates $B(T, X)$:

$$B(T_{i-1} + \tau, X) = \mathfrak{L}_\tau^{-1} \left\{ \frac{\hat{B}(\lambda, X)}{\lambda} \right\}. \tag{14}$$

This transform can be performed efficiently via the Stehfest algorithm:

$$B(T_{i-1} + \tau, X) = \sum_{k=1}^{N} \frac{St_k^N}{k} \hat{B}(k\Lambda, X), \quad \Lambda = \frac{\ln 2}{\tau}. \tag{15}$$

Choosing $N = 12$ is typically sufficient. Coefficients St_k^{12} are given below

1	2	3	4	5	6
$-0.01(6)$	$16.01(6)$	-1247	$27554.(3)$	$-263280.8(3)$	1324138.7
7	8	9	10	11	12
$-3891705.5(3)$	$7053286.(3)$	-8005336.5	5552830.5	-2155507.2	359251.2

It is obvious that these coefficients are very stiff. For small T inversion can be numerically unstable unless computation is carried with many significant digits. It is clear that equation (8) can be viewed as a special case of equation (15) with $N = 1$, $St_1^1 = 1$, and $\Lambda = 1/(T_i - T_{i-1})$.

The above procedure allows one to calculate $B(T_i, X_j)$ *for given* v_{ij}. To calibrate the model to the market, v_{ij} are changed until model and market prices agree. It is worth noting that, as always, vectorizing $\hat{B}(\lambda, X)$ makes computation more efficient.

The calibration algorithm is summarized as follows:

(A) At initialization, $B_0(X)$ given by equation (4) is computed on the spatial grid;

(B) At time T_{i+1}, given $B_i(X)$, equations (13) and (14) are used to compute $B(\lambda, X_j)$ and $B(T_i, X_j)$ at specified market strikes only; $\{v_{ij}\}$ are adjusted until model prices match market prices;

(C) After calibration at time T_{i+1} is complete, $B(T_i, X)$ is computed on the entire spatial grid using new model parameters at time T_{i+1};

(D) The algorithm is repeated for the next time slice.

If so desired, $B(T, X)$ can be calculated on the entire temporal-spatial grid with very limited additional effort.

For illustrative purposes a tiled local volatility model is calibrated to SX5E equity volatility data as of 01/03/2010. This data is taken from AH. Depending on maturity, one needs up to 13 tiles to be able to calibrate the model to the market. In Figure 1 model and market implied volatilities for the index are shown graphically, while in Table 1 the same volatilities are presented numerically. In Figure 2 the calibrated tiled local volatility is shown. In Figure 3, the Laplace transforms of the Green's functions $\hat{G}(\lambda, X_j, X')$ are shown as functions of X' for fixed λ. In Figure 4, the Laplace transforms of the Green's functions $\hat{G}(\lambda, X_j, X_j)$ are shown as functions of λ. In Figure 5, functions $B(T_i, X)$ are shown as functions of X. In all these Figures model parameters calibrated to the SX5E volatility surface are used.

To summarize, it is shown in this section that systematic application of the Laplace transform can be used to construct a calibration algorithm which is exact, fast, and robust.

5 Propagation problem with small number of tiles

In this section local volatility with either one or two tiles is considered and the corresponding propagation problem is solved via the Laplace transform. This is done in order to facilitate understanding of the general multi-tile set-up introduced earlier.

5.1 One-tile case

To start with, the one-tile case with $\sigma = \sigma_0$ is considered. Needless to say, this is the classical Black-Scholes case. In this case matrix equation (12) is trivial

$$\begin{pmatrix} -1 \\ -q_0 \end{pmatrix} \alpha_{0,+} + \begin{pmatrix} 1 \\ -q_0 \end{pmatrix} \alpha_{1,-} = \begin{pmatrix} 0 \\ -1 \end{pmatrix},$$

where

$$q_0 = \sqrt{\frac{2\lambda}{\sigma_0^2} + \frac{1}{4}}.$$

Accordingly, $\alpha_{0,+} = \alpha_{1,-} = 1/2q_0$, and the Green's function $\hat{G}(\lambda)$ and the corresponding option price $\hat{B}(\lambda)$ have the form

$$\hat{G}(\lambda, X, X') = \frac{e^{-q_0|X-X'|}}{q_0}.$$

$$\hat{B}(\lambda, X) = e^{-\frac{|X|}{2}} - \frac{e^{-q_0|X|}}{2q_0}.$$

The inverse Carson-Laplace transform of $\hat{B}(\lambda)$ yields the option price $B(T)$:

$$B(T, X) = e^{-\frac{|X|}{2}}\Phi\left(\frac{|X| - \frac{\sigma_0^2 T}{2}}{\sqrt{\sigma_0^2 T}}\right) + e^{\frac{|X|}{2}}\Phi\left(-\frac{|X| + \frac{\sigma_0^2 T}{2}}{\sqrt{\sigma_0^2 T}}\right).$$

Here and below $\Phi(\xi), \phi(\xi)$ are the cumulative density and density of the standard Gaussian variable.

While the above transforms can be computed in a closed form, in multi-tile case it is not possible. Accordingly, an approximation valid for $\lambda \to \infty$ is useful:

$$q_0 \approx \frac{\zeta}{\sigma_0} + \frac{\sigma_0}{8\zeta}, \qquad e^{-q_0|X|} \approx e^{-\frac{\zeta}{\sigma_0}|X|}\left(1 - \frac{\sigma_0|X|}{8\zeta}\right),$$

$$\hat{B}_a(\lambda, X) \approx e^{-\frac{|X|}{2}} - \frac{\sigma_0 e^{-\frac{\zeta}{\sigma_0}|X|}}{2\zeta} + \frac{\sigma_0^2|X|e^{-\frac{\zeta}{\sigma_0}|X|}}{16\zeta^2},$$

where $\zeta = \sqrt{2\lambda}$. It is well-known that for $z < 0$

$$\begin{array}{c} \mathcal{L}^{-1}\left(\frac{e^{\zeta z}}{\zeta^3}\right) = \sqrt{T}\Psi_3\left(\frac{z}{\sqrt{T}}\right), \\ \mathcal{L}^{-1}\left(\frac{e^{\zeta z}}{\zeta^4}\right) = T\Psi_4\left(\frac{z}{\sqrt{T}}\right), \end{array} \tag{16}$$

where

$$\begin{array}{c} \Psi_3(\xi) = \xi\Phi(\xi) + \phi(\xi), \\ \Psi_4(\xi) = \frac{1}{2}\left(\left(\xi^2+1\right)\Phi(\xi) + \xi\phi(\xi)\right). \end{array}$$

Equation (16) shows that the inverse Carson-Laplace transform of $\hat{B}_a(\lambda)$ yields an approximate option price:

$$B_a(T, X) = e^{-\frac{|X|}{2}} - \sigma_0\sqrt{T}\Psi_3\left(-\frac{|X|}{\sigma_0\sqrt{T}}\right) + \frac{\sigma_0^2 T|X|}{8}\Psi_4\left(-\frac{|X|}{\sigma_0\sqrt{T}}\right). \tag{17}$$

Exact and approximate implied volatilities for several representative maturities are shown in Figure 6. (It is clear that exact implied volatility is equal to σ_0.) This Figure shows that the above approximation is reasonably accurate provided that $\sigma_0^2 T$ is sufficiently small.

5.2 Two-tile case

In this section it is assumed that

$$\sigma(X)=\begin{cases}\sigma_0, & X\le\bar{X},\\ \sigma_1 & X>\bar{X}.\end{cases}$$

For concreteness, the case when $X<\bar{X}_0$ is considered. In the case in question equation (11) has the form

$$\begin{pmatrix}-1 & 1 & 1 & 0\\ -q_0 & q_0 & -q_0 & 0\\ 0 & -e^{q_0\left(\bar{X}_0-X\right)} & -e^{-q_0\left(\bar{X}_0-X\right)} & e^{-q_1\left(\bar{X}_0-X\right)}\\ 0 & -q_0e^{q_0\left(\bar{X}_0-X\right)} & +q_0e^{-q_0\left(\bar{X}_0-X\right)} & -q_1e^{-q_1\left(\bar{X}_0-X\right)}\end{pmatrix}\begin{pmatrix}\alpha_{0,+}\\ \alpha_{1,+}\\ \alpha_{1,-}\\ \alpha_{2,-}\end{pmatrix}=\begin{pmatrix}0\\ -1\\ 0\\ 0\end{pmatrix},$$

so that

$$=\begin{pmatrix}\alpha_{0,+} & \alpha_{1,+} & \alpha_{1,-} & \alpha_{2,-}\end{pmatrix}\\ =\begin{pmatrix}\frac{1}{2q_0}+\frac{(q_0-q_1)}{2q_0(q_0+q_1)}e^{-2q_0\left(\bar{X}_0-X\right)} & \frac{(q_0-q_1)}{2q_0(q_0+q_1)}e^{-2q_0\left(\bar{X}_0-X\right)} & \frac{1}{2q_0} & \frac{1}{(q_0+q_1)}e^{(q_1-q_0)\left(\bar{X}_0-X\right)}\end{pmatrix}$$

Accordingly, when $X>\bar{X}_0$, $\hat{G}(\lambda,X,X')$ can be written as

$$\hat{G}(\lambda,X,X')=\begin{cases}\frac{1}{2q_0}e^{-q_0\left|X'-X\right|}+\frac{(q_0-q_1)}{2q_0(q_0+q_1)}e^{q_0\left(X'+X-2\bar{X}_0\right)}, & X'\le\bar{X}_0,\\ \frac{1}{(q_0+q_1)}e^{-q_1\left(X'-\bar{X}_0\right)-q_0\left(\bar{X}_0-X\right)}, & \bar{X}_0<X'.\end{cases}$$

By the same token, when $X>\bar{X}_0$, it can be written as

$$\hat{G}(\lambda,X,X')=\begin{cases}\frac{1}{(q_0+q_1)}e^{q_1\left(\bar{X}_0-X\right)+q_0\left(X'-\bar{X}_0\right)}, & X'\le\bar{X}_0,\\ \frac{1}{2q_1}e^{-q_1\left|X'-X\right|}+\frac{(q_1-q_0)}{2q_1(q_1+q_0)}e^{-q_1\left(X'+X-2\bar{X}_0\right)}, & \bar{X}_0<X'.\end{cases}$$

As expected,

$$\hat{G}(\lambda,X,X')=\hat{G}(\lambda,X',X).$$

It can be shown either by using equation (13), or by direct calculation, that

$$\hat{B}(\lambda,X)=e^{-\frac{|X|}{2}}-\frac{(q(X)+q(0)-(q_0+q_1))e^{-q(X)\left|X-\bar{X}_0\right|-q(0)\left|\bar{X}_0\right|}}{2q(0)(q_0+q_1)}-\frac{e^{-q(X)\left(|X|-\left|\bar{X}_0\right|\right)-q(0)\left|\bar{X}_0\right|}}{(q(X)+q(0))}. \tag{18}$$

where

$$q(X)=\sqrt{\frac{2\lambda}{\sigma^2(X)}+\frac{1}{4}}=\begin{cases}\sqrt{\frac{2\lambda}{\sigma_0^2}+\frac{1}{4}}, & X\le\bar{X}_0,\\ \sqrt{\frac{2\lambda}{\sigma_1^2}+\frac{1}{4}}, & X>\bar{X}_0.\end{cases}$$

When $\lambda\to\infty$, $\hat{B}(\lambda,X)$ can be expanded as follows

$$\hat{B}(\lambda,X)=e^{-\frac{|X|}{2}}\\ -\frac{\left(\left(\frac{1}{\sigma(0)}+\frac{1}{\sigma(X)}\right)-\left(\frac{1}{\sigma_0}+\frac{1}{\sigma_1}\right)\right)}{\frac{2}{\sigma(0)}\left(\frac{1}{\sigma_0}+\frac{1}{\sigma_1}\right)\zeta}e^{-\left(\frac{\left|X-\bar{X}_0\right|}{\sigma(X)}+\frac{\left|\bar{X}_0\right|}{\sigma(0)}\right)\zeta}\left(1-\frac{\sigma(X)\left|X-\bar{X}_0\right|+\sigma(0)\left|\bar{X}_0\right|}{8\zeta}\right)\\ -\frac{1}{\left(\frac{1}{\sigma(0)}+\frac{1}{\sigma(X)}\right)\zeta}e^{-\left(\frac{|X|-\left|\bar{X}_0\right|}{\sigma(X)}+\frac{\left|\bar{X}_0\right|}{\sigma(0)}\right)\zeta}\left(1-\frac{\sigma(X)\left(|X|-\left|\bar{X}_0\right|\right)+\sigma(0)\left|\bar{X}_0\right|}{8\zeta}\right).$$

$$\hat{B}(\lambda, X) = e^{-\frac{|X|}{2}}$$
$$-\frac{\sigma(0)\left(\frac{\sigma_0\sigma_1(\sigma(0)+\sigma(X))}{\sigma(0)\sigma(X)}-(\sigma_0+\sigma_1)\right)}{2(\sigma_0+\sigma_1)\zeta}e^{-\left(\frac{|X-\bar{X}_0|}{\sigma(X)}+\frac{|\bar{X}_0|}{\sigma(0)}\right)\zeta}\left(1-\frac{\sigma(X)|X-\bar{X}_0|+\sigma(0)|\bar{X}_0|}{8\zeta}\right)$$
$$-\frac{\sigma(0)\sigma(X)}{(\sigma(0)+\sigma(X))\zeta}e^{-\left(\frac{|X|-|\bar{X}_0|}{\sigma(X)}+\frac{|\bar{X}_0|}{\sigma(0)}\right)\zeta}\left(1-\frac{\sigma(X)\left(|X|-|\bar{X}_0|\right)+\sigma(0)|\bar{X}_0|}{8\zeta}\right).$$

The inverse Carson-Laplace transform using on equation (16) yields

$$B(T,X) = e^{-\frac{|X|}{2}} - \sigma(0)\sqrt{T}\left(\frac{(\sigma_0+\sigma_1-2\sigma(0))}{(\sigma_0+\sigma_1)}\Psi_3\left(-\left(\frac{|X-\bar{X}_0|}{\sigma(X)\sqrt{T}}+\frac{|\bar{X}_0|}{\sigma(0)\sqrt{T}}\right)\right)\right.$$
$$\left.+\Psi_3\left(-\left(\frac{|X|-|\bar{X}_0|}{\sigma(X)\sqrt{T}}+\frac{|\bar{X}_0|}{\sigma(0)\sqrt{T}}\right)\right)\right)$$
$$+\frac{\sigma(0)\sigma(X)T}{8}\left(\frac{\left(\frac{\sigma_0\sigma_1(\sigma(0)+\sigma(X))}{\sigma(0)\sigma(X)}-(\sigma_0+\sigma_1)\right)\left(\sigma(X)|X-\bar{X}_0|+\sigma(0)|\bar{X}_0|\right)}{(\sigma_0+\sigma_1)\sigma(X)}\Psi_4\left(-\left(\frac{|X-\bar{X}_0|}{\sigma(X)\sqrt{T}}+\frac{|\bar{X}_0|}{\sigma(0)\sqrt{T}}\right)\right)\right.$$
$$\left.+\frac{2\left(\sigma(X)\left(|X|-|\bar{X}_0|\right)+\sigma(0)|\bar{X}_0|\right)}{(\sigma(0)+\sigma(X))}\Psi_4\left(-\left(\frac{|X|-|\bar{X}_0|}{\sigma(X)\sqrt{T}}+\frac{|\bar{X}_0|}{\sigma(0)\sqrt{T}}\right)\right)\right). \tag{19}$$

Figure 7 shows the implied volatility computed using the approximate formula (19) and the implied volatility computed by the exact algorithm using ????. This approximation provides adequate solution to the original problem. Note that the classical short-time approximation

$$\sigma_{imp}(X) = \frac{X}{\int_0^X \frac{d\xi}{\sigma_{loc}(\xi)}} = \frac{|X|}{\frac{|X|-|\bar{X}_0|}{\sigma(X)}+\frac{|\bar{X}_0|}{\sigma(0)}}, \tag{20}$$

is extremely inaccurate in the case under consideration.

6 Conclusions

In this paper a robust and exact algorithm for calibration of a tiled local volatility model to sparse market data is proposed. Its efficacy is illustrated by showing how to apply it for calibration of a tiled local volatility model to a particular set of sparse market data. It is shown that the algorithm generates a non-arbitrageable and well-behaved implied volatility surface for options on SX5E. Other applications of this and related algorithms will be reported elsewhere.

Acknowledgement 1 *Alex Lipton is a co-head and Artur Sepp is vice-president of the Global Quantitative Group at Bank of America Merrill Lynch. Productive conversations with several colleagues, including Leif Andersen, Stewart Inglis, Marsha Lipton, David Shelton and Charlie Wang, are gratefully acknowledged. Discussions and exchange of ideas with Jesper Andreasen were particularly important and very enjoyable. Email: alex.lipton@baml.com, artur.sepp@baml.com*

References

[1] Andersen L and R Brotherton-Ratcliffe, 1998 *The equity option volatility smile: a finite difference approach* Journal of Computational Finance 1(2), pages 5-38

[2] Andreasen J and N Huge, 2011a *Volatility interpolation* Risk, March, pages 76-79

[3] Andreasen J and N Huge, 2011b *Random grids* Risk, July, pages 62-67

[4] Ayache E, Henrotte P, Nassar S and X Wang, 2004 *Can anyone solve the smile problem* Wilmott, pages 78-96

[5] Blacher G 2001 *A new approach for designing and calibrating stochastic volatility models for optimal delta-vega hedging of exotic options* Global Derivatives Conference, Juan-les-Pins

[6] Brown G and C Randall, 1999 *If the skew fits* Risk, April, pages 62-65

[7] Coleman T, Li Y and A Verma, 1999 *Reconstructing the unknown local volatility function* Journal of Computational Finance, 2, pages 77-100

[8] Cox J, 1975 *Notes on option pricing I: constant elasticity of variance diffusions* Working Paper, Stanford University

[9] Derman E and I Kani, 1994 *The volatility smile and its implied tree* Goldman Sachs Quantitative Strategies Research Notes

[10] Dupire B, 1994 *Pricing with a smile* Risk, July, pages 18-20

[11] Hagan P, Kumar D, Lesniewski A and D Woodward, 2002 *Managing smile risk* Wilmott, pages 84-108

[12] Leij FJ and Th van Genuchten, 1995 *Approximate analytical solutions for solute transport in two-layer porous media* Transport in Porous Media, 18, pages 65-85

[13] Lipton A, 2001 *Mathematical Methods for Foreign Exchange: a Financial Engineer's Approach* World Scientific, Singapore.

[14] Lipton A, 2002 *The vol smile problem* Risk, February, pages 81-85

[15] Lipton A, 2011 *Three sources and three component parts of the Universal Volatility Model: theory and practice* Global Derivatives Conference, Paris

[16] Rubinstein M, 1983 *Displaced diffusion option pricing* Journal of Finance, 38, pages 213-217

[17] Rubinstein M, 1994 *Implied binomial trees* Journal of Finance, 49, pages 771-818

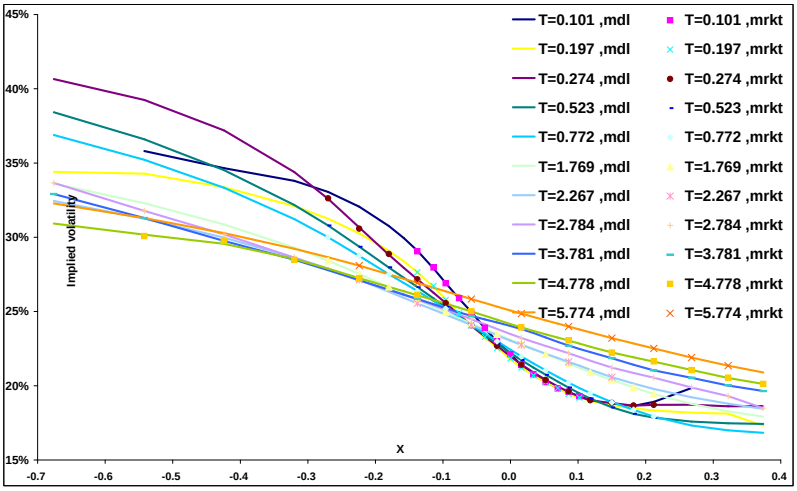

Figure 1: Market and model SX5E implied volatility quotes for March 1, 2010.

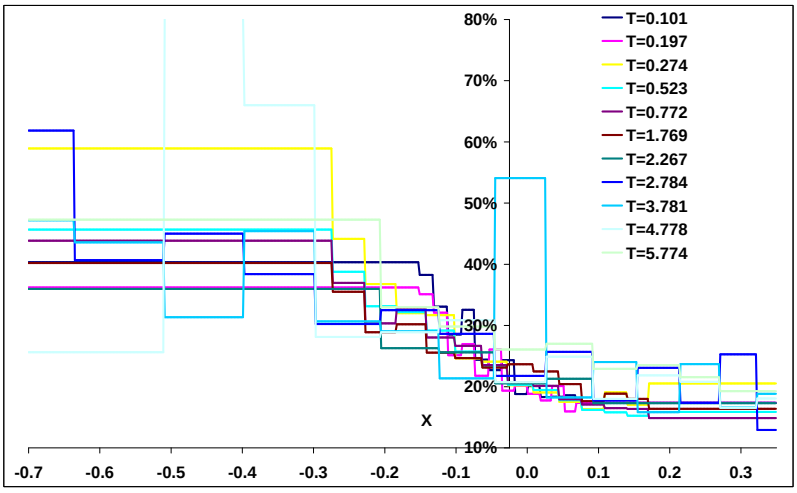

Figure 2: Calibrated local volatility for March 1, 2010.

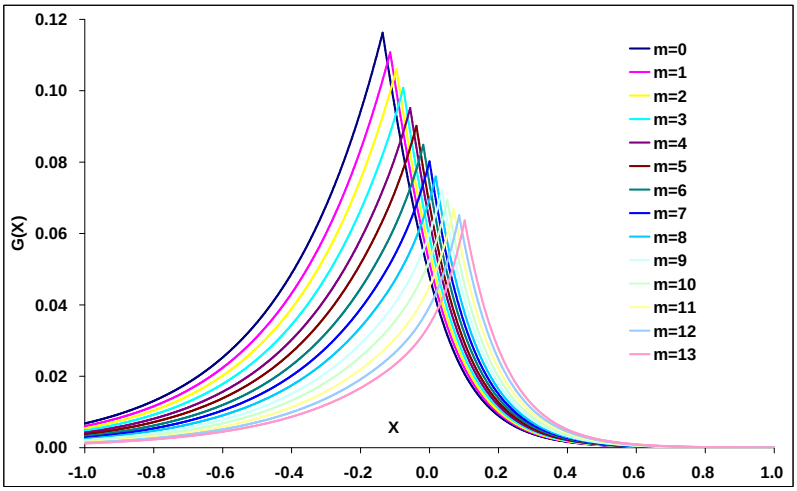

Figure 3: The Green's functions $\hat{G}_1(\lambda, X_j, X')$ as functions of X', where $\lambda = 1$ and $X = X_j$, $0 \leq j \leq 13$, are given in Table 1.

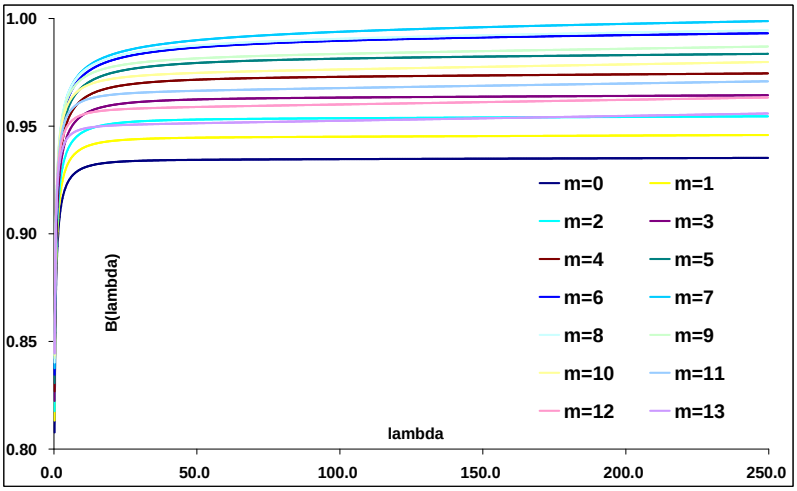

Figure 4: Option prices $\hat{B}(\lambda, X_j)$ as functions of λ, where X_j are given in Table 1.

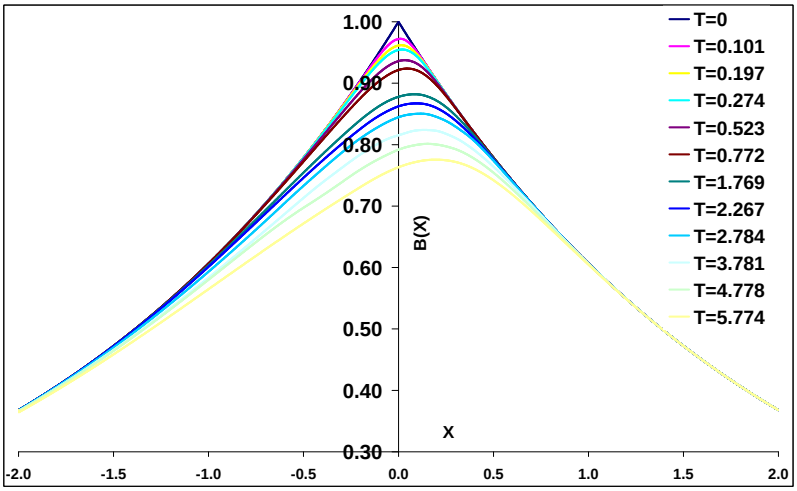

Figure 5: Option prices $B(T_i, X)$ as functions of X, where T_i are given in Table 1.

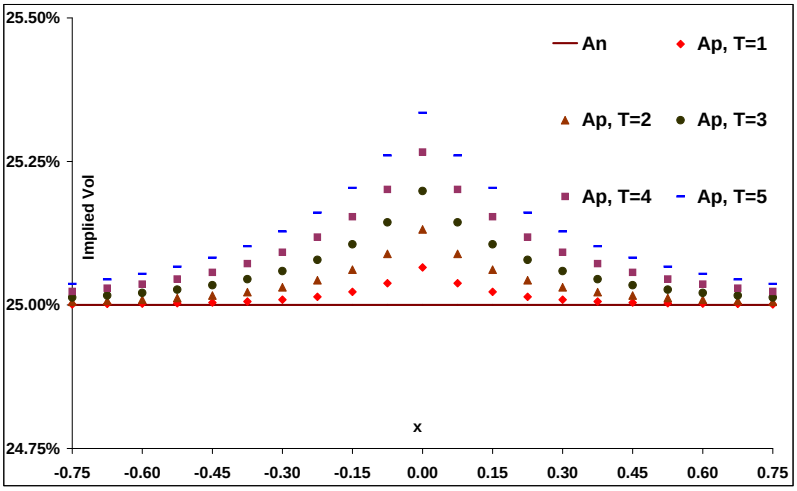

Figure 6: Implied volatility given by equation (17) with $\sigma_0 = 25\%$ vs. exact implied volatility σ_0.

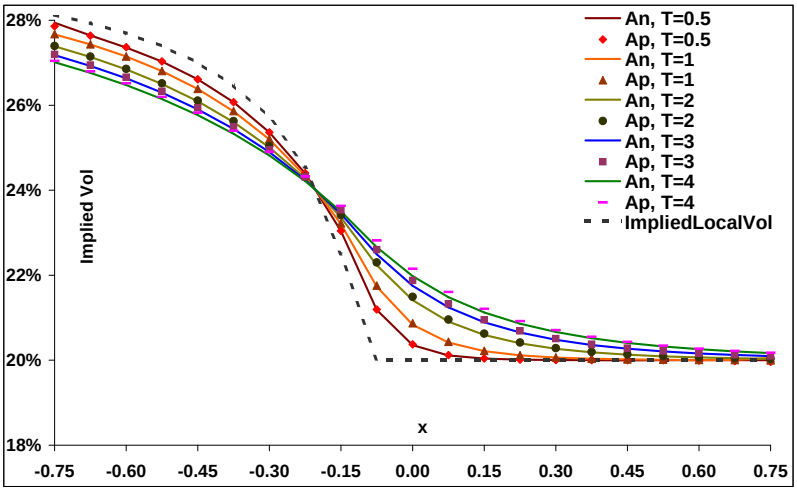

Figure 7: Two-tile case with $\sigma_0 = 30\%$, $\sigma_1 = 20\%$, $\bar{X}_0 = -0.1$. Implied volatility computed using equation (19) vs. implied volatility computed via the exact Carson-Laplace using equation (18); for five representative maturities $T = 1, ..., 5$. For comparison, implied volatility computed via equation (20) is shown as well.

K/T	0.101		0.197		0.274		0.523		0.772		1.769		2.267		2.784		3.781		4.778		5.774	
	mdl	mkt	mdl	mkt	mdl	mkt	mdl	mkt	mdl	mkt	mdl	mkt	mdl	mkt	mdl	mkt	mdl	mkt	mdl	mkt	mdl	mkt
51.31			34.40		40.66		38.42		36.88		33.62		32.44		33.66	33.66	32.91	32.91	30.92		32.27	
58.64	35.80		34.29		39.25		36.60		35.21		32.30		31.25		31.78	31.78	31.29	31.29	30.18	30.08	31.30	
65.97	34.65		33.37		37.20		34.52		33.34		30.86		29.98		30.19	30.19	29.76	29.76	29.56	29.75	30.28	
73.30	33.80		32.10		34.39		32.17		31.22		29.30		28.63		28.63	28.63	28.49	28.48	28.54	28.48	29.22	
76.97	33.05		31.25		32.59	32.62	30.79	30.79	30.00	30.01	28.42	28.43	27.89		27.83		27.78		27.88		28.66	
80.63	32.06		30.27		30.66	30.58	29.37	29.36	28.75	28.76	27.53	27.53	27.13	27.13	27.11	27.11	27.11	27.11	27.25	27.22	28.09	28.09
84.30	30.76		29.09		28.82	28.87	27.96	27.98	27.51	27.50	26.63	26.66	26.33		26.44		26.46		26.68		27.51	
86.13	29.95		28.38		27.94		27.27		26.92		26.19		25.92		26.11		26.14		26.36		27.20	
87.96	29.10	29.06	27.65	27.64	27.16	27.17	26.64	26.63	26.38	26.37	25.79	25.75	25.55	25.55	25.80	25.80	25.85	25.85	26.10	26.11	26.93	26.93
89.97	27.90	27.97	26.66	26.72	26.26		25.88		25.71		25.30		25.11		25.42		25.49		25.77		26.60	
91.63	26.92	26.90	25.82	25.78	25.57	25.57	25.30	25.31	25.20	25.19	24.93	24.97	24.79		25.12		25.23		25.53		26.36	
93.46	25.98	25.90	24.86	24.89	24.76		24.64		24.63		24.54		24.43		24.78		24.94		25.26		26.09	
95.29	24.98	24.88	24.08	24.05	24.04	24.07	24.06	24.04	24.11	24.11	24.19	24.18	24.10	24.10	24.48	24.48	24.71	24.69	25.00	25.01	25.84	25.84
97.12	23.86	23.90	23.24	23.29	23.31		23.41		23.53		23.81		23.73		24.14		24.46		24.71		25.57	
98.96	22.98	23.00	22.58	22.53	22.69	22.69	22.83	22.84	23.00	22.99	23.47	23.47	23.40		23.82		24.26		24.45		25.33	
100.79	22.14	22.13	21.78	21.84	21.97		22.20		22.42		23.11		23.03		23.48		24.03		24.15		25.07	
102.62	21.38	21.40	21.24	21.23	21.43	21.42	21.72	21.73	21.98	21.98	22.81	22.83	22.75	22.75	23.22	23.22	23.81	23.84	23.93	23.92	24.86	24.86
104.45	20.78	20.76	20.70	20.69	20.89		21.22		21.50		22.48		22.45		22.85		23.55		23.69		24.63	
106.29	20.24	20.24	20.23	20.25	20.40	20.39	20.74	20.74	21.04	21.04	22.15	22.13	22.16		22.68		23.25		23.47		24.41	
108.12	19.84	19.82	19.86	19.84	19.95		20.28		20.59		21.81		21.87		22.43		22.95		23.24		24.19	
109.95	19.57	19.59	19.45	19.44	19.58	19.62	19.87	19.88	20.20	20.22	21.50	21.51	21.61	21.61	22.19	22.19	22.71	22.69	23.04	23.05	23.99	23.99
111.78	19.28	19.29	19.18	19.20	19.26		19.49		19.84		21.20		21.35		21.94		22.48		22.84		23.79	
113.62	19.04		18.98		19.01	19.02	19.13	19.14	19.50	19.50	20.91	20.91	21.08		21.69		22.27		22.63		23.60	
117.28	18.73		18.68		18.84	18.85	18.55	18.54	18.90	18.88	20.39	20.39	20.58	20.58	21.22	21.22	21.85	21.86	22.24	22.23	23.21	23.21
120.95	18.65		18.48		18.66	18.67	18.11	18.11	18.38	18.39	19.89	19.90	20.14		20.86		21.41		21.91		22.84	
124.61	18.92		18.34		18.71	18.71	17.85	17.85	17.92	17.93	19.45	19.45	19.79		20.54	20.54	21.03	21.03	21.62	21.64	22.51	22.51
131.94	19.85		18.19		18.72		17.59		17.32		18.77		19.22		19.88	19.88	20.54	20.54	21.06	21.05	21.90	21.90
139.27			18.12		18.61		17.47		17.00		18.29		18.79		19.30	19.30	20.02	20.02	20.53	20.54	21.35	21.35
146.60			17.31		18.63		17.43		16.83		17.92		18.44		18.49	18.49	19.64	19.64	20.12	20.12	20.90	

Figure 8: Table 1. The table shows market and model SX5E implied volatility quotes for March 1, 2010. Expiries range from one week to six years and strikes range from 50-150% of the current spot of 2,772. Market data is clearly very sparse. The same market data has been used by AH.